Alloy Engineering of Defect Properties in Semiconductors: Suppression of Deep Levels in Transition-Metal Dichalcogenides

Bing Huang,[1,2,3] Mina Yoon,[3] Bobby G. Sumpter,[3,4] Su-Huai Wei,[5] and Feng Liu[2]
[1]*Beijing Computational Science Research Center, Beijing 100094, China*
[2]*Department of Materials Science and Engineering, University of Utah, Salt Lake City, Utah 84112, USA*
[3]*Center for Nanophase Materials Sciences, Oak Ridge National Laboratory, Oak Ridge, Tennessee 37831, USA*
[4]*Computer Science and Mathematics Division, Oak Ridge National Laboratory, Oak Ridge, Tennessee 37831, USA*
[5]*National Renewable Energy Laboratory, Golden, Colorado 80401, USA*
(Received 15 May 2015; published 18 September 2015)

Developing practical approaches to effectively reduce the amount of deep defect levels in semiconductors is critical for their use in electronic and optoelectronic devices, but this still remains a very challenging task. In this Letter, we propose that specific alloying can provide an effective means to suppress the deep defect levels in semiconductors while maintaining their basic electronic properties. Specifically, we demonstrate that for transition-metal dichalcogenides, such as $MoSe_2$ and WSe_2, where anion vacancies are the most abundant defects that can induce deep levels, the deep levels can be effectively suppressed in $Mo_{1-x}W_xSe_2$ alloys at low W concentrations. This surprising phenomenon is associated with the fact that the band edge energies can be substantially tuned by the global alloy concentration, whereas the defect level is controlled locally by the preferred locations of Se vacancies around W atoms. Our findings illustrate a concept of alloy engineering and provide a promising approach to control the defect properties of semiconductors.

DOI: 10.1103/PhysRevLett.115.126806 PACS numbers: 73.20.Hb, 68.55.Ln, 73.22.-f

The application of semiconductors in electric and optoelectronic devices depends critically on controlling their band structures and defect properties. While band structures of semiconductors have been successfully tuned by strain [1,2] or alloy engineering [3], there is still a lack of effective methods to control the defect properties, especially to suppress the in-gap deep levels, in semiconductors [4]. The deep-level defects, which can act as scattering centers to decrease carrier mobilities or charge recombination centers to reduce carrier lifetime, are easier to form and have an even stronger impact in low-dimensional systems [5–7]. Based on the experiments of monolayer transition-metal dichalcogenides MX_2 ($M = \mathrm{W}$, Mo; $X = \mathrm{S}$, Se), it has been found that anion vacancies are the most abundant defects [8–11] that can induce in-gap deep levels and significantly degrade the performance for advanced electronic and optoelectronic devices [8–13].

In the past, two main approaches have been developed to reduce the amount of deep levels in semiconductors by introducing additional dopants. The first approach involves the design of defect complexes by inducing foreign dopants to suppress the deep-level defects through donor-acceptor level repulsion [4,14], but its efficiency strongly depends on the symmetries of donor-acceptor levels and the solubility of the foreign dopants [15,16]. The second requires creation of passivated impurity bands to modify the host band structure near band edges that may make deep levels shallower [4,17–19], but the basic electronic structure of the host material can also be significantly changed, leading to additional problems. Thus, it is highly desirable to develop new approaches to suppress the amount of deep levels in semiconductors while at the same time maintain the electronic properties of the host materials. In this Letter, we propose such an approach based on specific alloying.

Alloying has been mostly applied for band gap engineering of semiconductors, as the band gap of an alloy can be continually tuned as a function of alloy concentration. Here we take alloying to a new front in the engineering of defect properties of semiconductors. The basic concept is illustrated in Fig. 1. We assume that compounds A and B have similar structural or electronic properties and a strong type-II band alignment. Their similar structural or electronic

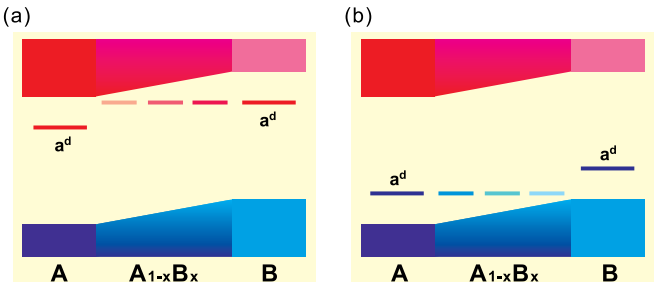

FIG. 1 (color online). Schematic plot of the concept for suppressing in-gap deep a^d levels in semiconducting A and B compounds by alloying. Two different typical situations are considered: (a) the a^d levels are closer to the CBM than the VBM in A and B, and (b) the a^d levels are closer to the VBM than the CBM in A and B.

properties ensure a high miscibility of A and B as well as maintain the same electronic properties independent of alloy concentration. On the other hand, a harmful defect D_h, which can induce a deep in-gap level a^d in A, will also induce a similar deep in-gap level a^d in B because of their similarity. If B has higher band edge energy than A, the band edge positions of $A_{1-x}B_x$ will increase as a function of x. Usually, the wave function of a deep level is very localized and most of the contribution comes from its nearest-neighbor atoms around the defect. The local environment of D_h in $A_{1-x}B_x$ can be classified into three different situations: (1) same as compound A (D_{h-A}), (2) same as compound B (D_{h-B}), and (3) the mixing of compounds A and B (D_{h-AB}). Ideally, the absolute energy positions of a^d for D_{h-A} (D_{h-B}) in $A_{1-x}B_x$ can be similar to that of a^d in the A (B) compound, assuming that the wave function of D_h is sufficiently localized. When the a^d levels in A and B are closer to the conduction band minimum (CBM) than the valence band maximum (VBM), as shown in Fig. 1(a), the a^d levels could become shallower with respect to CBM in $A_{1-x}B_x$ as x decreases, if D_h in $A_{1-x}B_x$ prefers to form as D_{h-B}. This could be true for empty levels, as it costs less energy for creating empty a^d levels of D_{h-B} at higher energy positions (with respect to the CBM) in $A_{1-x}B_x$. The D_{h-B} in $A_{1-x}B_x$ induces a locally deep a^d level in terms of the local B environment, however, as the global CBM position of $A_{1-x}B_x$ decreases as the x decreases. Consequently, the smaller x is in $A_{1-x}B_x$, the shallower the a^d level becomes with respect to the CBM. When the deep levels a^d in A and B are closer to the VBM rather than the CBM [Fig. 1(b)], the a^d level could become shallower in $A_{1-x}B_x$ as x increases, if the D_h in $A_{1-x}B_x$ prefers to form as D_{h-A}. This might also be achieved for the occupied levels, as it costs less energy for creating occupied a^d levels of D_{h-A} at lower energy positions (with respect to the VBM) in $A_{1-x}B_x$.

We selected the extensively studied MX_2 as a typical example to demonstrate our concept. $MoSe_2$ and WSe_2 have very similar electronic and defect properties, so that alloying them together to form $Mo_{1-x}W_xSe_2$ will not change their basic electronic structures. Importantly, the largely tunable band edge positions and the preferred formation sites of V_{Se} around W atoms in $Mo_{1-x}W_xSe_2$ make it possible to control their defect levels by alloying. The defect levels of Se vacancy (V_{Se}), which are very deep in both $MoSe_2$ and WSe_2, indeed become much shallower in $Mo_{1-x}W_xSe_2$ at low W concentrations, whereas the electronic structure is very similar to that of $MoSe_2$ (WSe_2).

In an ideal random alloy $Mo_{1-x}W_xSe_2$, the Se atom is surrounded by three metal atoms and the probability of finding a Se site with the first-neighbor motif $Mo_{3-n}W_n$ is $p_n(x) = C_3^n x^n (1-x)^{3-n}$. To simulate the ideal random alloy $Mo_{1-x}W_xSe_2$, we constructed seven special quasirandom structures [20] with different W concentrations ($x = 0.125$, 0.25, 0.375, 0.5, 0.625, 0.75, and 0.875) in a large 12×12 supercell. In constructing special quasirandom structures, the interatomic correlation functions of short-range pairs and triplets are required to be the same as ideal random alloys. The first-principles density functional theory, as implemented in the VASP package [21], is used for structural relaxation and electronic structure calculations. The projector augmented wave method in conjunction with the generalized gradient approximation within the framework of Perdew-Burke-Ernzerhof is adopted for the electron exchange and correlation. The kinetic energy cutoff for the plane wave basis is set to 350 eV. The Γ-centered 3×3 k-point mesh is used for the Brillouin zone integration, which ensures the total energies converged to within 1 meV/atom. A slab containing 15 Å vacuum region in the normal direction is used to simulate isolated 2D materials. All the structures are fully relaxed until the force on each atom is less than 0.01 eV/Å.

The synthesis of MX_2 alloys has been investigated recently, mostly for the purpose of band gap engineering [22–27]. Because of the same crystalline structure and lattice constant for the end-point constituents ($a = 3.315$ Å for $MoSe_2$, $a = 3.313$ Å for WSe_2), $Mo_{1-x}W_xSe_2$ alloys have negligible variations of the lattice constant (~0.06%) over the entire concentration range, as shown in Fig. 2(a). The electronic structures of $MoSe_2$ and WSe_2 are also almost the same in terms of the band dispersion and band gap [28]. The calculated band gaps of $MoSe_2$ and WSe_2 are 1.45 and 1.56 eV, respectively, close to the experimentally

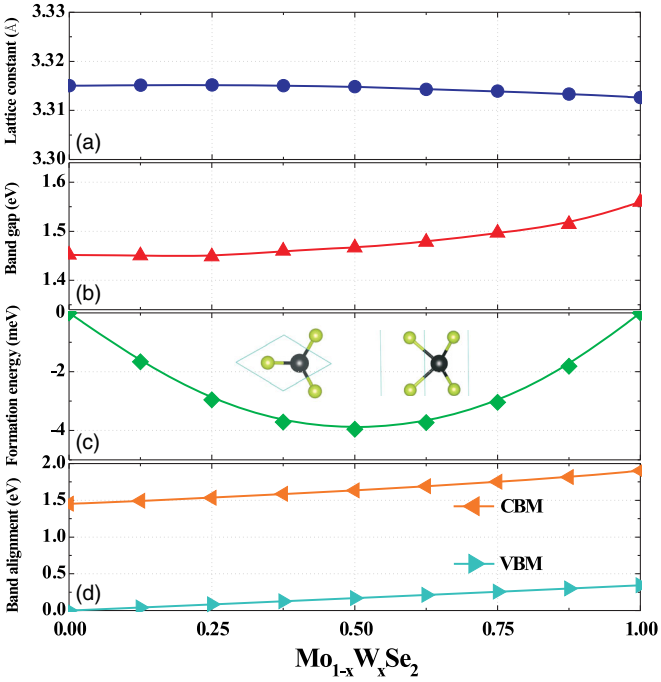

FIG. 2 (color online). The (a) in-plane lattice constant, (b) electronic band gap, (c) alloy formation energy, and (d) band alignments of $Mo_{1-x}W_xSe_2$ as a function of x. Inset: the top and side views of $MoSe_2$ (WSe_2) in the unit cell. The black atoms are the cation while the green atoms are the anion.

measured values ($E_g = 1.56$ eV for $MoSe_2$, $E_g = 1.65$ eV for WSe_2) [25,26]. The band gap of $Mo_{1-x}W_xSe_2$ does not monotonically depend on the W concentrations. As shown in Fig. 2(b), the band gap of $Mo_{1-x}W_xSe_2$ slightly decreases at $x < 0.25$ and then increases at $x > 0.25$, consistent with experimental observations [26]. The band gap bowing equation $E_g(x) = xE_g(WSe_2) + (1-x)E_g(MoSe_2) - bx(1-x)$ [3] can describe the deviation of band gap values from linearity, with a fitted coefficient $b = 0.15$ eV, agreeing well with the experimental measured value (~0.151 eV) [26]. Because of the perfectly matched lattice constants and very similar electronic structures, the alloy formation energies of $Mo_{1-x}W_xSe_2$ are slightly negative ($0 < x < 1$) compared to that of $MoSe_2$ and WSe_2 due to the slightly increased attractive Coulomb interaction (the different atomic orbital energy and electronegativity of Mo and W can give rise to a ~0.1e different charge state between them based on the Bader charge analysis), as shown in Fig. 2(c). This indicates no miscibility gap in the entire W concentration, again consistent with the experimental observations [22,25–27]. In $MoSe_2$ (WSe_2), its VBM is mostly contributed by the bonding d_{xy} and $d_{x^2+y^2}$ states of cation atoms, while its CBM is mostly contributed by the nonbonding d_{z^2} states of cation atoms. Because W 5d states have higher orbital energies than Mo 4d states [29], the band edges of WSe_2 are higher in energy than that of $MoSe_2$. As shown in Fig. 2(d), the band edge positions of $Mo_{1-x}W_xSe_2$ increase as a function of x, and the CBM (VBM) edge of $Mo_{1-x}W_xSe_2$ can be dramatically tuned by 0.45 (0.34) eV from $x = 0$ to $x = 1$.

Obviously, $Mo_{1-x}W_xSe_2$ is an ideal example to examine our concept [Fig. 1(a)] in terms of the large tunable band alignment. Because anion vacancy is the most abundant and harmful defect in MX_2, it is interesting to investigate whether or not the deep levels of V_{Se} can be suppressed in $Mo_{1-x}W_xSe_2$. The formation energy (and transition energy level) of a V_{Se} is mainly determined by its local environment, i.e., first-neighbor motif, because of the wave function localization of V_{Se}. The first-neighbor motif around a V_{Se} in $Mo_{1-x}W_xSe_2$ can be three Mo atoms (V_{Se-3Mo}), two Mo and one W atoms ($V_{Se-2Mo1W}$), one Mo and two W atoms ($V_{Se-1Mo2W}$), or three W atoms (V_{Se-3W}). We have performed calculations to confirm that the formation energies of V_{Se} with the same first-neighbor motif have a similar value independent of location [30]. However, the formation energies depend strongly on the choices of the first-neighbor motif, as shown in Fig. 3; the more W atoms in its first-neighbor motif, the lower the formation energy of a V_{Se}. The average formation energy of V_{Se-3W} is ~0.06, ~0.12, and ~0.18 eV lower than that of $V_{Se-1Mo2W}$, $V_{Se-2Mo1W}$, and V_{Se-3Mo}, respectively. Thus, V_{Se} is found preferably to form as V_{Se-3W} in $Mo_{1-x}W_xSe_2$ alloys.

The defect levels of V_{Se} around Fermi level in $MoSe_2$ (WSe_2) can be classified as one single a and two nearly

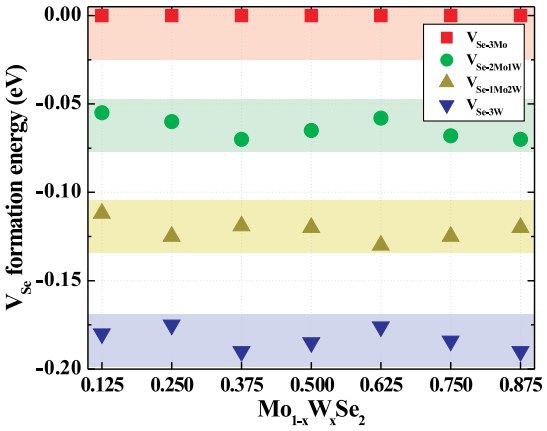

FIG. 3 (color online). The relative formation energies of anion vacancy V_{se} in $Mo_{1-x}W_xSe_2$ at seven different W concentrations x. In each $Mo_{1-x}W_xSe_2$, the formation energies of V_{se} at all the nonequivalent sites are calculated and classified into four groups in terms of their first-neighbor motifs around V_{se}, i.e., V_{Se-3Mo}, $V_{Se-2Mo1W}$, $V_{Se-1Mo2W}$, and V_{Se-3W}. The average formation energy of V_{se} with the same first-neighbor motif is plotted in this figure.

degenerate e states under C_{3v} symmetry. The a state, which is occupied based on the electron counting rule and resides inside the valence band (~0.25 eV below VBM), has negligible impact on the electronic structure of $MoSe_2$ (WSe_2). The e states, in contrast, are mostly contributed by the mixed d orbitals of the cation atoms around V_{Se} and are very deep inside the band gap, as shown in Figs. 4(a) and 4(b). In our calculations, the e states are 0.45 and 0.41 eV below the CBM of $MoSe_2$ and WSe_2, respectively, which are harmful for device operation because they can act as traps for the free carrier.

Based on our proposed concept [Fig. 1(a)], it should be possible to suppress the deep e levels in $Mo_{1-x}W_xSe_2$ at low W concentrations, because of the preferred location of V_{Se} as V_{Se-3W} and the much lower CBM position of $MoSe_2$ than WSe_2. To confirm this, we have systematically studied the defect states of V_{Se} at different sites in $Mo_{0.75}W_{0.25}Se_2$. We find that the energy positions of the in-gap e levels solely depend on their first-neighbor motifs, because of the strong charge localization of e levels (left inset of Fig. 4). Generally, the more W atoms that are in its first-neighbor motif, the shallower the e states will be close to alloy CBM, exactly as predicted by our model analysis (Fig. 1).

For the case of V_{Se-3Mo}, the e levels are very deep, about 0.45 eV below its CBM, the same as V_{Se} in $MoSe_2$. For the case of $V_{Se-2Mo1W}$, because the local symmetry around $V_{Se-2Mo1W}$ is broken, the e states are split into two states. The average energy separation between these two states and the CBM is 0.36 eV, which is shallower than that of V_{Se-3Mo}. For the case of $V_{Se-1Mo2W}$, the average distance between these two levels and the CBM decreases to 0.26 eV. Finally, for the case of V_{Se-3W}, which is energetically most stable, the energy difference between the e

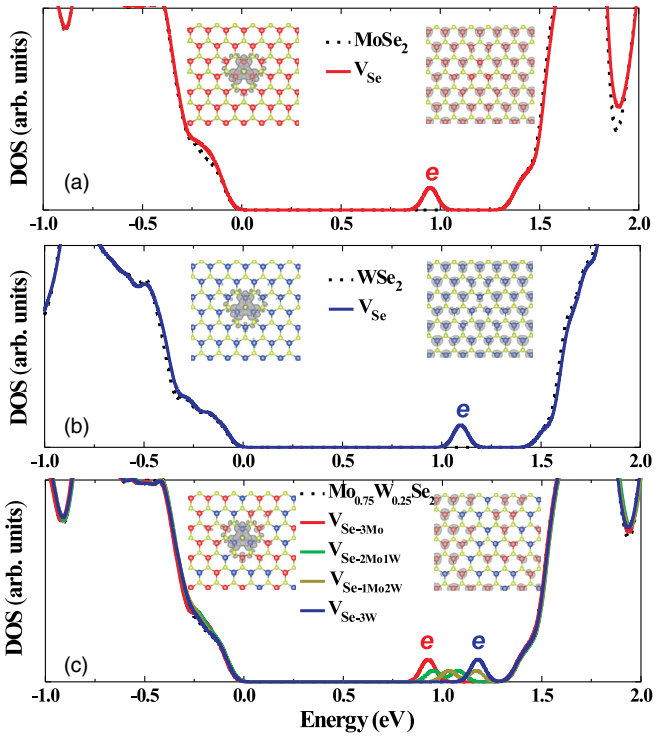

FIG. 4 (color online). The electronic density of states (DOS) of (a) $MoSe_2$, (b) WSe_2, and (c) $Mo_{0.75}W_{0.25}Se_2$ with (solid line) and without (dashed line) a V_{Se}. These DOSs have been aligned with the 1s core level of the host materials. The Fermi level is set to zero. Left inset: the charge densities of the in-gap e levels of V_{Se} in $MoSe_2$, WSe_2, and $Mo_{0.75}W_{0.25}Se_2$ (V_{Se-3W}). Right inset: the charge densities of the CBM in $MoSe_2$, WSe_2, and $Mo_{0.75}W_{0.25}Se_2$. It should be noted that only partial areas of charge densities around V_{Se} are shown here.

states and CBM is significantly reduced to 0.17 eV. This is dramatically different from that of V_{Se} in WSe_2, even though they have the same local chemical environment [left inset of Figs. 4(b) and 4(c)]. This is quite interesting because the basic electronic structure of $Mo_{0.75}W_{0.25}Se_2$ and $MoSe_2$ are almost the same in terms of the band gap and band dispersion [28], but their defect properties are dramatically different. Generally, it costs less energy for creating unoccupied e^d levels at higher energy positions [4,6]; thus, this electronic effect can explain the trend of formation energy difference of V_{Se} with different first-neighbor motifs (Fig. 3). We point out that our conclusion is not affected by more advanced hybrid functional calculations [28].

It is interesting to further clarify the physical origin of this deep to shallow transition of V_{Se} levels in $Mo_{0.75}W_{0.25}Se_2$. As mentioned above, the CBM states of $MoSe_2$ (WSe_2) are dominated by the nonbonding d_{z^2} orbitals of cation atoms with the wave functions extended perpendicular to the 2D plane; as a result, the strength of the wave function overlap between different cation atoms is not strong [right inset of Figs. 4(a) and 4(b)]. Because of the higher orbital energies of $5d_{z^2}$ (W) than $4d_{z^2}$ (Mo), combining with the weak intercation interaction, the CBM of $Mo_{0.75}W_{0.25}Se_2$ is largely contributed by the low-energy

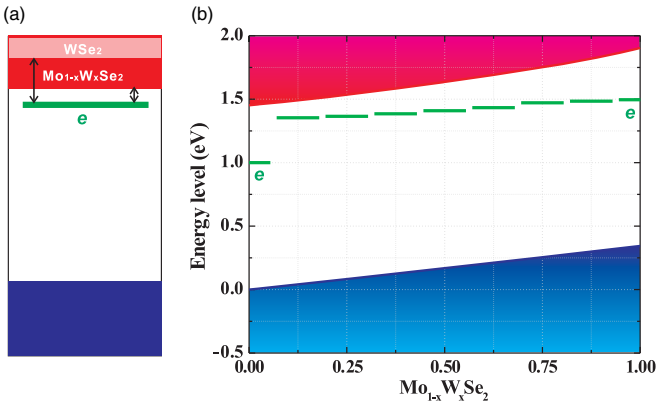

FIG. 5 (color online). (a) A schematic drawing of the in-gap e levels of V_{Se} (V_{Se-3W}) in $Mo_{1-x}W_xSe_2$. The in-gap e levels are locally deep in terms of the local WSe_2 environment but globally shallow in terms of the CBM of $Mo_{1-x}W_xSe_2$. (b) The calculated average energy positions of in-gap e levels (at the ground state configuration of V_{Se}) in $Mo_{1-x}W_xSe_2$ as a function of x.

Mo states (with small amount of W states), as shown by the CBM charge densities [right inset of Fig. 4(c)] [28]. The local environment of V_{Se-3W} [left inset of Fig. 4(c)] is similar to that of V_{Se} in WSe_2 [left-inset of Fig. 4(b)]; thus, it will induce locally deep e levels in terms of the local WSe_2 environment [Fig. 5(a)]. The global CBM of $Mo_{0.75}W_{0.25}Se_2$, however, is determined by the Mo states with lower orbital energy; as a result, the e levels of V_{Se-3W} become much shallower in $Mo_{0.75}W_{0.25}Se_2$.

Based on our design concept, the V_{Se-3W} e levels should become shallower at lower W concentrations in $Mo_{1-x}W_xSe_2$. Indeed, our calculations show that the absolute energy positions of V_{Se-3W} e levels in $Mo_{1-x}W_xSe_2$ are similar to that of V_{Se} in WSe_2 [Fig. 5(b)], but the significant changes of the CBM position in $Mo_{1-x}W_xSe_2$ as a function of x make the in-gap e levels much shallower at lower W concentrations. For example, the e levels are 0.13 eV below CBM in $Mo_{0.875}W_{0.125}Se_2$ compared to that of 0.45 eV below CBM in $MoSe_2$, and these levels are expected to be ~0.1 eV below CBM at dilute W concentrations based on the trend of e levels, which means that the carrier density can be enhanced by 5 orders of magnitude at room temperature. This enhanced carrier density generally leads to a significant improvement in device performance [31]. The sudden change of V_{Se} e level positions at $x \sim 0$ is the result of the sudden change of V_{Se} ground state configuration from V_{Se-3Mo} to V_{Se-3W} at $x \sim 0$. Clearly, our results also demonstrate that the introduction of a small amount of W in $MoSe_2$ will significantly suppress the deep e levels of V_{Se} in $MoSe_2$, but will not change its electronic structure. Our results may help rationalize the puzzling experimental observation that the carrier mobilities of $Mo_{1-x}W_xSe_2$ alloys increase monotonically when the W concentration continuously decreases from $x = 1$ to $x = 0.14$, even though the changes of the band gap and carrier effective mass are very small ($<6\%$).

We want to emphasize that the concept, which is utilizing the fact that some physical properties depend on the global concentration of the alloy whereas the other depends only on local concentration of the alloy, can have broad applications in improving doping properties, e.g., defect structure, solubility, and defect levels, of compounds through alloying. Our approach is not just unique to $MoSe_2/WSe_2$ systems, as we demonstrate for other members in the MX_2 family [28]. Generally, it can be readily applied to those alloy systems with similar host electronic properties and lattice parameters. This is important because the alloys made from similar electronic structure and lattice parameter materials usually have many advantages for specific applications in practice, such as very good solid solution and unchanged host electronic structures. In principle, our proposed approach can also be further extended to systems with dissimilar host electronic properties and lattice parameters, as long as the desired defect property tuning can be achieved, while the average host electronic properties remain useful and the strain induced phase separation can be effectively suppressed [32].

In conclusion, we have developed a concept to suppress the deep levels in semiconductors while maintaining the electronic properties of the host materials via specific alloying. This concept was demonstrated for the case of $Mo_{1-x}W_xSe_2$ materials. Since our concept is based on a general working principle, it may be widely applied to suppress the deep levels in other semiconductors via alloying, as long as good solid solutions without phase separation and tunable band edge positions can be achieved in these alloys.

B. H. acknowledges support from the Chinese Youth 1000 Talents Program. The work at Oak Ridge National Laboratory was conducted at the Center for Nanophase Materials Sciences, a DOE office of science user facility. The research at Utah and National Renewable Energy Laboratory was supported by the U.S. Department of Energy (Grant No. DE-FG02-04ER46148).

[1] D. Yu, Y. Zhang, and F. Liu, Phys. Rev. B **78**, 245204 (2008).
[2] Z. Liu, J. Wu, W. Duan, M. G. Lagally, and F. Liu, Phys. Rev. Lett. **105**, 016802 (2010).
[3] S.-H. Wei and A. Zunger, Phys. Rev. Lett. **76**, 664 (1996).
[4] *Advanced Calculations for Defects in Materials: Electronic Structure Methods*, edited by A. Alkauskas, P. Deak, J. Neuge-bauer, A. Pasquarello, and C. G. Van deWalle (Wiley, Weinheim, Germany, 2011).
[5] J. Li, S.-H. Wei, and L.-W. Wang, Phys. Rev. Lett. **94**, 185501 (2005).
[6] J. R. Chelikowsky, M. M. G. Alemany, T.-L. Chan, and G. M. Dalpian, Rep. Prog. Phys. **74**, 046501 (2011).
[7] D. Wang, D. Han, X. B. Li, S. Y. Xie, N. K. Chen, W. Q. Tian, D. West, H. B. Sun, and S. B. Zhang, Phys. Rev. Lett. **114**, 196801 (2015).
[8] W. Zhou, X. Zou, S. Najmaei, Z. Liu, Y. Shi, J. Kong, J. Lou, P. M. Ajayan, B. I. Yakobson, and J.-C. Idrobo, Nano Lett. **13**, 2615 (2013).
[9] H. Qiu, T. Xu, Z. Wang, W. Ren, H. Nan, Z. Ni, Q. Chen, S. Yuan, F. Miao, F. Song, G. Long, Y. Shi, L. Sun, J. Wang, and X. Wang, Nat. Commun. **4**, 2642 (2013).
[10] S. Tongay, J. Suh, C. Ataca, W. Fan, A. Luce, J. S. Kang, J. Liu, C. Ko, R. Raghunathanan, J. Zhou, F. Ogletree, J. Li, J. C. Grossman, and J. Wu, Sci. Rep. **3**, 2657 (2013).
[11] Y. Lin, T. Bjorkman, H. Komsa, P. Teng, C. Yeh, F. Huang, K. Lin, J. Jadczak, Y. Huang, P. Chiu, A. V. Krasheninnikov, and K. Suenaga, Nat. Commun. **6**, 6736 (2015).
[12] H.-P. Komsa and A. V. Krasheninnikov, Phys. Rev. B **91**, 125304 (2015).
[13] J.-Y. Noh, H. Kim, and Y.-S. Kim, Phys. Rev. B **89**, 205417 (2014).
[14] A. Janotti, S.-H. Wei, and S. B. Zhang, Appl. Phys. Lett. **83**, 3522 (2003).
[15] S.-H. Wei and S. B. Zhang, Phys. Rev. B **66**, 155211 (2002).
[16] D. Segev and S.-H. Wei, Phys. Rev. Lett. **91**, 126406 (2003).
[17] Z. Teukam *et al.*, Nat. Mater. **2**, 482 (2003).
[18] M. Joseph, H. Tabata, and T. Kawai, Jpn. J. Appl. Phys. **38**, L1205 (1999).
[19] Y. Yan, J. Li, S.-H. Wei, and M. M. Al-Jassim, Phys. Rev. Lett. **98**, 135506 (2007).
[20] A. Zunger, S.-H. Wei, L. G. Ferreira, and J. E. Bernard, Phys. Rev. Lett. **65**, 353 (1990).
[21] G. Kresse and J. Furthmüller, Comput. Mater. Sci. **6**, 15 (1996).
[22] D. O. Dumcenco, H. Kobayashi, Z. Liu, Y. Huang, and K. Suenaga, Nat. Commun. **4**, 1351 (2013).
[23] Y. Gong *et al.*, Nano Lett. **14**, 442 (2014).
[24] H. Li *et al.*, J. Am. Chem. Soc. **136**, 3756 (2014).
[25] S. Tongay *et al.*, Appl. Phys. Lett. **104**, 012101 (2014).
[26] M. Zhang *et al.*, ACS Nano **8**, 7130 (2014).
[27] Y. Chen, J. Xi, D. O. Dumcenco, Z. Liu, K. Suenaga, D. Wang, Z. Shuai, Y. Huang, and L. Xie, ACS Nano **7**, 4610 (2013).
[28] See Supplemental Material at http://link.aps.org/supplemental/10.1103/PhysRevLett.115.126806 for the band structures of $MoSe_2$, WSe_2, and $Mo_{1-x}W_xSe_2$ alloys; the hybrid functional calculations of V_{Se} in $Mo_{1-x}W_xSe_2$; and the case of suppression of deep levels in the $Mo_{1-x}W_xS_2$ alloys.
[29] W. A. Harrison, *Electronic Structure and The Properties of Solids* (Dover Publications, Mineola, NY, 1989).
[30] The formation energy of a V_{Se} is defined as $E_f = E(\text{defect}) - E(\text{perfect}) + \mu_{Se}$. $E(\text{defect})$ and $E(\text{perfect})$ represent the total energy of a 12×12 supercell with and without one V_{Se}, respectively. μ_{Se} is the chemical potential of a Se atom. Here, we focus on the E_f differences of a V_{Se} at different sites, which is independent of the choice of μ_{Se}.
[31] S. Chen, A. Walsh, X. G. Gong, and S.-H. Wei, Adv. Mater. **25**, 1522 (2013).
[32] X. B. Niu, G. B. Stringfellow, and F. Liu, Phys. Rev. Lett. **107**, 076101 (2011).